



# Ratiometric fluorescence chemosensors for copper(II) and mercury(II) based on FRET systems

Guangjie He, Xiaolin Zhang<sup>\*</sup>, Cheng He, Xiuwen Zhao, Chunying Duan<sup>\*</sup>

State Key Laboratory of Fine Chemicals, Dalian University of Technology, Dalian 116012, China

## ARTICLE INFO

### Article history:

Received 23 May 2010

Received in revised form 6 September 2010

Accepted 14 September 2010

Available online 21 September 2010

### Keywords:

Chemosensor

FRET

Rhodamine

Coumarin

## ABSTRACT

A system based on FRET mechanism, comprising a coumarin donor and a rhodamine acceptor, was developed for the selective and quantitative detection of metal ions. Fluorescent chemosensors **RCs**, linked by 1,2-diethylamine, exhibit significant fluorescence enhancement and excellent selectivity toward  $\text{Cu}^{2+}$ . Fluorescent probes **CRB** and **CR6G**, linked by hydrazide, function as ratiometric receptors for  $\text{Cu}^{2+}$  chromogenically and fluorogenically in organic-aqueous media. Furthermore, the characteristic rhodamine-based fluorescence response of **CRB** (excitation at 550 nm) exhibits high selectivity for  $\text{Hg}(\text{II})$ . The construction of this kind of universal FRET system opens a broader prospect for future design of ratiometric fluorescent probes.

© 2010 Published by Elsevier Ltd.

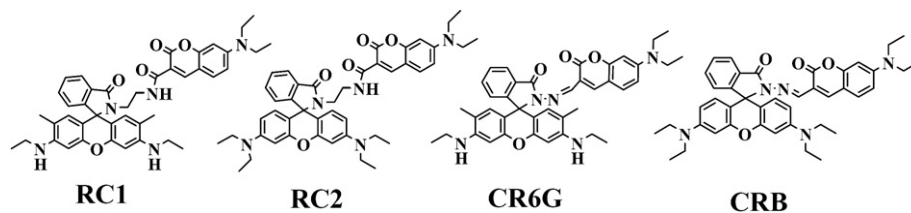
## 1. Introduction

The development of molecular fluorescent sensors for detection of environmentally and biologically important species has always been of particular importance and usually involves the design and synthesis of molecules that contain binding sites and signaling subunits to be able to display selective changes in fluorescence emission upon guest binding.<sup>1</sup> For heavy and transition-metal ions, specifically paramagnetic  $\text{Cu}^{2+}$ , selective sensory protocols are particularly critical, because copper is an essential trace element acted as a cofactor for many fundamental biological processes in all currently known life forms, but alternations in its cellular homeostasis are connected to serious neurodegenerative diseases.<sup>2</sup> And because of its essential yet toxic nature, cells exert strict control over intracellular copper distributions and thermodynamically estimated level of free copper ions in the cytoplasm lies well below a single ion per cell.<sup>3</sup> Accordingly, highly sensitive optical imaging with copper-selective fluorescent sensors is strongly demanded, for visualizing kinetically labile copper with subcellular resolution at the molecular level.<sup>4</sup> However, since the divalent copper ion is a well-known efficient fluorescence quencher in the most case, fluorescence enhancement for copper binding is fairly faint and therefore poses a significant design

challenge.<sup>5</sup> Since the simply changing of fluorescence intensity arising to the metal-binding tends to be interfered by various factors, such as instrumental efficiency, environmental conditions, and the probe concentration,<sup>6</sup> the simultaneous recording of the fluorescence intensities at two wavelengths and calculation of their ratio thus is one of the attractive approaches in this field and provides a built-in correction to eliminate most or all of the ambiguities.<sup>7</sup> In this regards, the using of guest-induced fluorescence resonance energy transfer (FRET) mechanism should be an efficient approach to design ratiometric fluorescence probes, since they can emit at two different wavelengths at a single excitation source.<sup>8</sup>

The important practical challenge to achieving this approach is selectivity of suitable 'Donor–Acceptor' pair, because a requirement for Förster energy transfer is that the emission spectrum of the donor must overlap with the absorption spectrum of the acceptor.<sup>9</sup> Owing to their excellent photochemical and photophysical properties,<sup>10</sup> rhodamine and coumarin derivatives have often been used as effective optical probes for detecting different species. And at the time coumarin moiety has been used as an energy donor,<sup>10a</sup> obvious change of absorption spectrum induced by target molecules, from Leuco derivatives with unconjugated structures to ring-opened tautomer, makes rhodamine-based dyes very suitable for FRET acceptor.<sup>11</sup> In this regard, a kind of practical and universal FRET system to realize simultaneous selective and quantitative detection of copper(II) ions was developed, mainly because of the good complexation ability for metal ions and simply synthesis procedures (Scheme 1).<sup>12</sup>

<sup>\*</sup> Corresponding authors. Tel.: +86 411 8370 2355; fax: +86 411 3989 3830; e-mail addresses: [zhangxiaolin@dlut.edu.cn](mailto:zhangxiaolin@dlut.edu.cn) (X. Zhang), [cyduan@dlut.edu.cn](mailto:cyduan@dlut.edu.cn) (C. Duan).

Scheme 1. Structure of the receptors **RC1**, **RC2**, **CRB**, and **CR6G**.

### 1.1. Synthesis and spectral properties of **RC1**

Compound **RC1** was synthesized according to the literature.<sup>13</sup> The characteristic peak of the 10-carbon near 65 ppm in <sup>13</sup>C NMR spectra suggests that the spirolactam ring form of **RC1** exists dominantly in solution. Single crystal X-ray structural analysis confirms the coexistence of two fluorophores in **RC1**, where the rhodamine 6G moiety exhibits a luminescence-inactive ring-closed tautomeric form. It could be found that there was a weak intramolecular  $\pi \cdots \pi$  interaction between the phenyl rings of rhodamine 6G xanthene part and the coumarin (dihedral angle and distance of the two phenyl rings being 4.4° and 3.54 Å), respectively, which caused the two fluorophores within one molecular stacking in a close parallel pattern, allowing a possible FRET progress between the two chromophores. **RC1** is yellow and fluorescence inactive in solution. Free **RC1** displays an absorption band that arises from coumarin chromophore in the visible region centered at 415 nm, which is confirmed by the absorption spectrum of the reference material 7-diethylamino-2-oxo-2H-chromen-3-carboxylic acid. The spirolactam form of the rhodamine moiety only absorbs UV radiation and shows a band at about 302 nm.

Upon addition of  $\text{Cu}(\text{ClO}_4)_2$  to the solution of **RC1** ( $\log \varepsilon_{\text{cou}}=4.64$ ), a new absorption band at 525 nm appeared in the visible range and increased gradually and then remained constant ( $\log \varepsilon_{\text{rho}}=4.68$ ) after approximately 1 equiv of  $\text{Cu}^{2+}$  being added (Fig. 1). Accordingly, the titration solution exhibited an obvious and characteristic color change from yellow to pink, indicating that probe **RC1** could serve as a 'naked-eye' indicator for  $\text{Cu}^{2+}$ . The presence of several isosbestic points reflects the existence of only one intermediate complex.<sup>14</sup> The linear fitting of the titration curve reveals a 2:1 stoichiometry of the **RC1**– $\text{Cu}^{2+}$  complexation species with the association constant of  $2.66 \times 10^{12}$ . The fluorescent spectrum of **RC1** upon the addition of  $\text{Cu}(\text{ClO}_4)_2$  was shown in Fig. 1. For the free ligand, upon excitation at 415 nm, a strong emission at 460 nm was observed, which could be attributed to the coumarin energy donor unit ( $\Phi_{\text{f(cou)}}=0.25$ ).<sup>13</sup> Upon stepwise adding  $\text{Cu}^{2+}$ , the fluorescence intensity of coumarin donor at 460 nm decreased successively, and new emission of rhodamine 6G acceptor around 550 nm appeared and developed remarkably.

As mentioned above, the UV–vis titration demonstrated that the copper-binding could induce the opening of the spirolactam ring in **RC1** and result in an absorbance band at about 525 nm. Thus, upon the gradual addition of  $\text{Cu}^{2+}$ , the overlapping between the emission spectra of the energy donor (coumarin chromophore) and the absorption spectra of the energy acceptor (rhodamine chromophore) increased, which would greatly enhance the intra-molecular FRET process and lead to significant fluorescence enhancement of rhodamine 6G moiety at 550 nm ( $\Phi_{\text{f(rho)}}=0.34$ ). The overall effect upon addition of 2 equiv of  $\text{Cu}^{2+}$  made the ratio of rhodamine-to-coumarin type emission intensities ( $F_{550}/F_{460}$ ) upon excitation at 415 nm vary from 0.06 to 14.8, about 250-fold emission ratio increase due to FRET modulation (the FRET efficiency could be calculated as 90%).<sup>15</sup> The presence of a sharp isosbestic point might suggest that the two luminescence bands are isogenicus.

To further explore the availability of **RC1** as a highly selective probe for  $\text{Cu}^{2+}$ , absorbance and fluorescent spectra of **RC1** response to other metal ions that probably affect the fluorescence intensity were examined (Fig. S1 and S2). No significant spectral changes were observed for **RC1** (20  $\mu\text{M}$ ) in the presence of alkali-, alkaline-earth metals, such as  $\text{Na}^+$ ,  $\text{K}^+$ ,  $\text{Mg}^{2+}$ ,  $\text{Ca}^{2+}$  and the first-row transition metals  $\text{Mn}^{2+}$ ,  $\text{Fe}^{2+}$ ,  $\text{Co}^{2+}$ ,  $\text{Ni}^{2+}$ ,  $\text{Zn}^{2+}$ ,  $\text{Cd}^{2+}$  as well as  $\text{Pb}^{2+}$  and  $\text{Ag}^+$  (10 equiv), respectively. The presence of  $\text{Hg}^{2+}$  (10 equiv) caused a similar fluorescence enhancement at 550 nm, but a little fluorescence intensity decrease at 460 nm with the  $F_{550}/F_{460}$  value only up to 0.75. Furthermore, the competition experiments revealed that the  $\text{Cu}^{2+}$ -induced ratiometric fluorescence response was unaffected in the presence of the metal cations mentioned above. Even the presence of  $\text{Hg}^{2+}$  only induced little interference with  $\text{Cu}^{2+}$ -induced ratiometric fluorescence response. Thus the  $\text{Cu}^{2+}$ -selective binding and FRET-ON response could take place in the coexistence of the competitive metal ions. Furthermore, the response of **RC1** to  $\text{Cu}^{2+}$  was reversible rather than a cation-catalyzed reaction.<sup>16</sup> The absorption and fluorescence signals of rhodamine group in the **RC1**– $\text{Cu}^{2+}$  complexation species disappeared instantly upon the addition of EDTA. When excess  $\text{Cu}^{2+}$  was added in, the signals would be recovered.

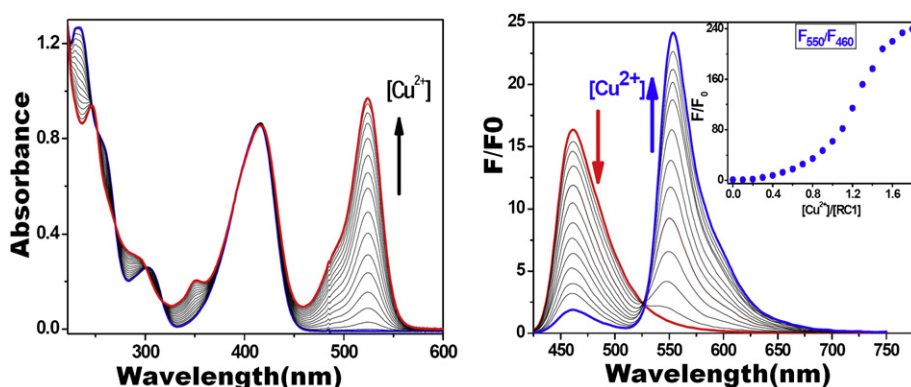


Fig. 1. Left: UV–vis absorption spectra of **RC1** (20  $\mu\text{M}$ ) in  $\text{CH}_3\text{CN}$  upon gradual addition of  $\text{Cu}(\text{ClO}_4)_2$ . Right: Fluorescence response of **RC1** (20  $\mu\text{M}$ ) upon the addition of  $\text{Cu}(\text{ClO}_4)_2$ . Inset: titration profiles of **RC1** (20  $\mu\text{M}$ ) upon addition of  $\text{Cu}^{2+}$  showing the fluorescence intensities at 460 nm and 550 nm with an excitation at 415 nm.

Since the free ligand **RC1** was relatively flexible,  $\text{Cu}^{2+}$  should be easy to fit into the pseudo cavity formed between the two carbonyl groups of coumarin and rhodamine 6 G units. IR spectra of **RC1** and **RC1**– $\text{Cu}^{2+}$  complex exhibited that the peak at  $1684\text{ cm}^{-1}$  corresponding to the characteristic amide carbonyl absorption of the rhodamine unit<sup>17</sup> was shifted to a lower wavenumber ( $1610\text{ cm}^{-1}$ ) upon addition of  $\text{Cu}^{2+}$ . At the same time, the stretching band at  $1699\text{ cm}^{-1}$  corresponding to the carbonyl group of the coumarin moiety was shifted. It is assumed that both the carbonyl groups of the rhodamine and coumarin units participated in the coordination. Furthermore, the peak at  $3348\text{ cm}^{-1}$  that could be attributed to the imine N–H stretching vibration of H–N–C=O group, fade out upon addition of  $\text{Cu}^{2+}$ , implying the possible deprotonation of amide group during the coordination to  $\text{Cu}^{2+}$ . The fourth coordination site of  $\text{Cu}^{2+}$  may be occupied by the counter-anion  $\text{ClO}_4^-$ . With careful investigation, one may note that when  $\text{Cu}^{2+}$  was added to **RC1**, the enhancement of absorbance at 525 nm was much more significant than that of fluorescence intensity at 550 nm. However, the ring opening of the spirolactam form of rhodamine derivatives generally results in comparable amplifications of absorption and fluorescence signals. Thus, it seems that binding of  $\text{Cu}^{2+}$  did open the spirolactam ring, but at the same time, the fluorescence of the ring-opened amide form was probably partially quenched by  $\text{Cu}^{2+}$ . The quenching mechanism may be similar to that of some  $\text{Cu}^{2+}$  probes displaying fluorescence quenching for the paramagnetic nature of the copper ion.<sup>18</sup> From a sensitivity viewpoint, it was preferable to inhibit this quenching effect to generate a more notable fluorescence enhancement.

## 1.2. The comparison of FRET efficiency RC1 and RC2

To investigate how the FRET efficiency is influenced by the overlap between the emission spectrum of the donor and the absorption spectrum of the acceptor so as to modulate the ratio of FRET, the UV–vis and fluorescent titrations of **RC2** target  $\text{Cu}^{2+}$  were also performed. Upon gradual addition of  $\text{Cu}(\text{ClO}_4)_2$  to the solution of **RC2** (20  $\mu\text{M}$ ) in  $\text{CH}_3\text{CN}$  ( $\log \varepsilon_{\text{cou}}=4.64$ ,  $\Phi_{\text{f(cou)}}=0.29$ ), a new absorption band centered around 550 nm (Fig. S3) appeared in the visible range and increased gradually and remained constant after approximately 1 equiv of  $\text{Cu}^{2+}$  being added ( $\log \varepsilon_{\text{rho}}=4.66$ ,  $\Phi_{\text{f(rho)}}=0.27$ ). By contrast with **RC1**, there was about 25 nm red shift in the maximum absorption peak of **RC2**. The fluorescent titration experiment of **RC2** upon the addition of  $\text{Cu}(\text{ClO}_4)_2$  was also presented in Fig. S3. The overall effect upon addition of about 2 equiv of  $\text{Cu}^{2+}$  was a 1.6-fold quenching of fluorescence at 460 nm and a 48-fold enhancement at 585 nm. The ratio of rhodamine-to-coumarin type emission intensities ( $F_{585}/F_{460}$ ) upon excitation at 415 nm varied from 0.018 to 1.42, about 80-fold emission ratio

increase due to FRET modulation (the FRET efficiency could be calculated as 33%).

As discussed above, it could be deduced that the FRET efficiency of **RC1** was about three times higher than that of **RC2**, indicating that **RC1** was more sensitive than **RC2** for the detection of  $\text{Cu}^{2+}$ . From a point of the mechanism of FRET, about 25 nm red shift in the maximum absorption peak of **RC2** compared with that of **RC1** leading to the spectra overlap between the acceptor and donor of **RC1** was larger than that of **RC2** (Fig. S4), which resulted that the FRET efficiency of **RC1** was higher than that of **RC2**.

## 1.3. Syntheses and spectral properties of CRB and CR6G

To further test the practicability and popularity of this universal FRET system based on coumarin and rhodamine, carbohydrazone block was selected as connection of donor and acceptor due to its simplicity of syntheses in the design of **CRB** and **CR6G**. The introduction of coumarin group through C=N bond would not only benefit the coumarin functioning as emit donor through red shift the fluorescence for better overlap the absorption spectrum of rhodamine donors, but also enhance the coordination capacity of the sensors toward the copper ion. **CRB** and **CR6G** were synthesized from the reaction of rhodamine hydrazide with 7-diethylamino-coumarin-3-aldehyde. The characteristic peak of the 10-carbon at 65.77 ppm shown in  $^{13}\text{C}$  NMR spectrum suggests that the spirolactam form of **CRB** and **CR6G** exist predominantly in solution.<sup>12a,19</sup> Such a special conformation of the rhodamine group gives a yellow color and fluorescence inactivity of compounds **CRB** and **CR6G** in solutions.

Free **CRB** displays absorption bands of coumarin chromophore in the visible region centered at 454 nm ( $\log \varepsilon=4.64$ ), which is confirmed by the absorption spectra of the reference 7-diethylamino-coumarin-3-aldehyde. The spirolactam form of the rhodamine moiety of **CRB** absorbs the UV light and shows a band at about 250 nm. Upon addition of  $\text{Cu}(\text{ClO}_4)_2$  in the  $\text{CH}_3\text{CN}/\text{H}_2\text{O}$  (9:1, v/v) solution of **CRB** (20  $\mu\text{M}$ ), two new absorption bands centered around 495 and 550 nm in the visible range appeared, developed and finally remained constant ( $\log \varepsilon=4.86$  and  $\log \varepsilon=4.95$ , respectively) after approximately 5 equiv of  $\text{Cu}^{2+}$  were added (Fig. 2). The former should be assigned to coumarin chromophore with significant bathochromic shift due to the  $\text{Cu}^{2+}$ -binding, while the latter could be attributed to the formation of the ring-opened tautomer of the rhodamine chromophore. Accordingly, the titration solution exhibits an obvious and characteristic color change from yellow to red, indicating that probe **CRB** can serve as a ‘naked-eye’ indicator for  $\text{Cu}^{2+}$  ion. The individual profile of the titration curve at 495 nm assumes a 2:1 stoichiometry for the **CRB**– $\text{Cu}^{2+}$  complexation species with an association constant of  $6.50\pm0.20\times10^{10}\text{ M}^{-2}$ .

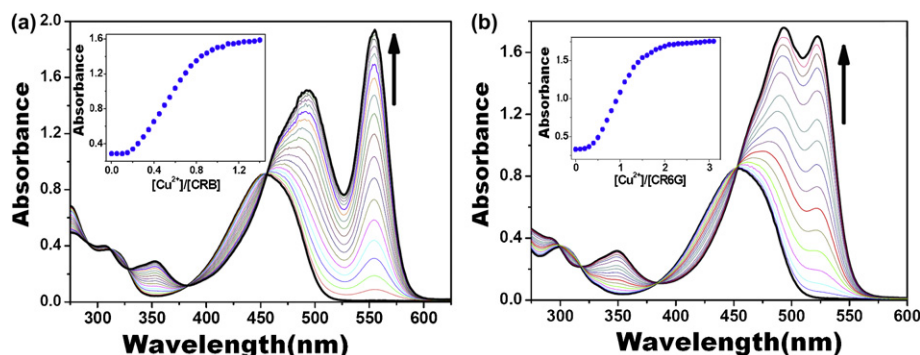


Fig. 2. UV–vis spectra of **CRB** (20  $\mu\text{M}$ ) (a) and **CR6G** (20  $\mu\text{M}$ ) (b) in  $\text{CH}_3\text{CN}/\text{H}_2\text{O}$  (9:1, v/v) upon addition of different concentrations of  $\text{Cu}(\text{ClO}_4)_2$ . The insets exhibit the absorbance of 495 nm as a function of  $[\text{Cu}^{2+}]$ .

The presence of several isosbestic points reveals the existence of only one intermediate complex.<sup>14</sup>

The absorption spectral changes of **CR6G** on addition of copper ions were shown in Fig. 2. Upon addition of  $\text{Cu}(\text{ClO}_4)_2$  to the solution of **CR6G** (20  $\mu\text{M}$ ) in the  $\text{CH}_3\text{CN}/\text{H}_2\text{O}$  (9:1, v/v) ( $\log \varepsilon=4.63$ ), two new absorption bands centered around 495 nm and 525 nm appeared in the visible range and increased gradually and remained constant after approximately 3 equiv of  $\text{Cu}^{2+}$  being added. The color change is obvious from yellow to orange before and after addition of  $\text{Cu}^{2+}$ , indicating that **CR6G** can serve as a ‘naked-eye’ indicator for  $\text{Cu}^{2+}$ . The individual profile of the titration curve at 495 nm assumes a 2:1 stoichiometry for the **CR6G**– $\text{Cu}^{2+}$  complexation species with an association constant of  $6.08 \pm 0.20 \times 10^{10} \text{ M}^{-2}$ .

Importantly, no significant absorbance enhancement around 495 nm was observed in the presence of 10 equiv of other transition-metal ions, such as  $\text{Mn}^{2+}$ ,  $\text{Fe}^{2+}$ ,  $\text{Co}^{2+}$ ,  $\text{Ni}^{2+}$ , and group 12 ions  $\text{Zn}^{2+}$ ,  $\text{Cd}^{2+}$  as well as  $\text{Pb}^{2+}$  and  $\text{Ag}^+$ , implying that **CRB** and **CR6G** could have special binding ability toward  $\text{Cu}^{2+}$  (Fig. S5, cyan bars). Furthermore, the competition experiments of **CRB** (20  $\mu\text{M}$ ) in  $\text{CH}_3\text{CN}/\text{H}_2\text{O}$  (9:1, v/v) by adding 0.2 mM equiv of other metal cations and succeeding 50  $\mu\text{M}$  of  $\text{Cu}^{2+}$  revealed that the spectroscopic responses were unaffected in the presence of alkali-, alkaline-earth, and transition-metal ions (Fig. S5, blue bars).

The fluorescence response of **CRB** when excited at 420 nm corresponding to the excitation wavelength of coumarin group was also conducted (Fig. 3). Upon the addition of  $\text{Cu}(\text{ClO}_4)_2$  in the  $\text{CH}_3\text{CN}/\text{H}_2\text{O}$  (9:1, v/v) solution of **CRB** (20  $\mu\text{M}$ ) and excited at 420 nm, the emission band with the maximum emission wavelength at 518 nm corresponding to the typical emission of coumarin group decreased and finally leveled off after approximate 2 equiv of  $\text{Cu}^{2+}$  were added. As discussed above, the fluorescence quenching of coumarin moiety by  $\text{Cu}^{2+}$  ion could also be ascribed to a d–d electron paramagnetic quenching or/and an energy transfer mechanism.<sup>18</sup> The fluorescence response of **CR6G** when excited at

420 nm corresponding to the excitation wavelength of coumarin group was also conducted (Fig. 3). The emission band peaked at 516 nm decreased and finally almost disappeared after 1 equiv of  $\text{Cu}^{2+}$  were added.

IR spectra of **CRB** and **CRB**– $\text{Cu}^{2+}$  complexation species exhibited that the peak at  $1690 \text{ cm}^{-1}$  corresponding to the characteristic amide carbonyl absorption of rhodamine unit of free **CRB**,<sup>20</sup> was shifted to a lower wavenumber ( $1648 \text{ cm}^{-1}$ ) upon the complexation of  $\text{Cu}^{2+}$ . At the same time, the  $\text{Cu}^{2+}$ -binding of **CRB** lead to the stretching band at  $1718 \text{ cm}^{-1}$  corresponding to the carbonyl group of coumarin in free **CRB** shifted to  $1707 \text{ cm}^{-1}$ . In this case, both the carbonyl groups of the rhodamine and coumarin units were considered to participate the chelating coordination.

The response of **CRB** (20  $\mu\text{M}$ ) to  $\text{Hg}(\text{ClO}_4)_2$  in UV–vis spectra in  $\text{CH}_3\text{CN}/\text{H}_2\text{O}$  (9:1, v/v) was also investigated. Upon addition of  $\text{Hg}(\text{ClO}_4)_2$  in the  $\text{CH}_3\text{CN}/\text{H}_2\text{O}$  (9:1, v/v) solution of **CRB** (20  $\mu\text{M}$ ), a new absorption band centered around 560 nm in the visible range appeared, developed, and finally remained constant ( $\log \varepsilon=4.81$ ) after approximately 3 equiv of  $\text{Hg}^{2+}$  were added (Fig. 4). The individual profile of the titration curve at 560 nm assumes a 1:1 stoichiometry for the **CRB**– $\text{Hg}^{2+}$  complexation species with an association constant of  $1.89 \times 10^5 \text{ M}^{-1}$ . Accordingly, the titration solution exhibits an obvious and characteristic color change from yellow to red, which should be assigned to the formation of the ring-opened tautomer of the rhodamine chromophore. However, no band around 495 nm was observed.

As is well-known, highly selective probes for  $\text{Hg}^{2+}$ , which give positive responses rather than fluorescent quenching upon analyte binding, are usually preferred to promote the sensitivity. Upon the addition of  $\text{Hg}(\text{ClO}_4)_2$  into the  $\text{CH}_3\text{CN}/\text{H}_2\text{O}$  (9:1, v/v) solution of **CRB** (20  $\mu\text{M}$ ), a new emission band centered at 585 nm (with an excitation wavelength at 550 nm, the typical excitation wavelength of rhodamine group) developed and finally attained an equilibrium after about 4 equiv of  $\text{Hg}^{2+}$  were added (Fig. 4,  $\Phi_F=0.43$ ). The typical

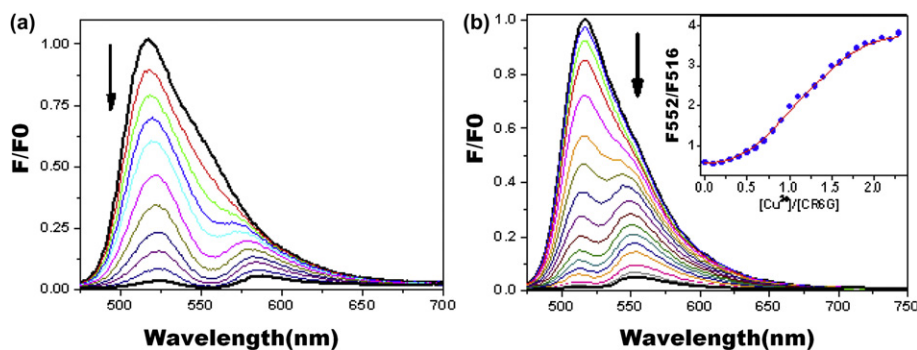


Fig. 3. (a) Fluorescence spectra of **CRB** (20  $\mu\text{M}$ ) and (b) **CR6G** in  $\text{CH}_3\text{CN}/\text{H}_2\text{O}$  (9:1, v/v) solution upon addition of increasing concentrations of  $\text{Cu}(\text{ClO}_4)_2$  with an excitation at 420 nm.

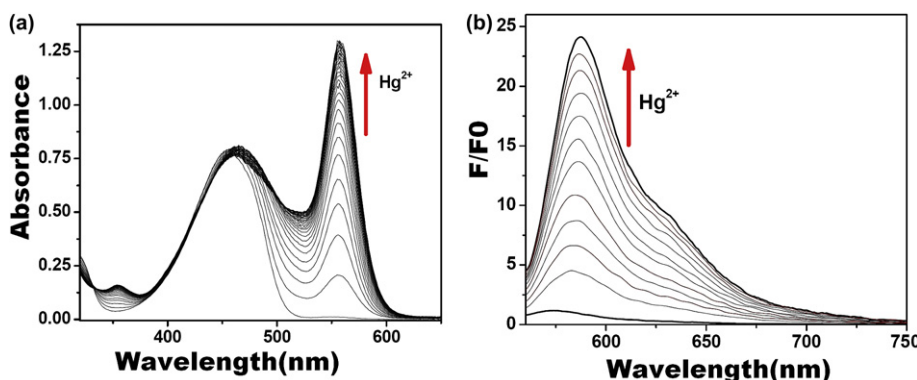


Fig. 4. (a) UV–vis spectra of **CRB** (20  $\mu\text{M}$ ) in  $\text{CH}_3\text{CN}/\text{H}_2\text{O}$  (9:1, v/v) solution upon addition of increasing concentrations of  $\text{Hg}(\text{ClO}_4)_2$ . (b) Fluorescence spectra of **CRB** (20  $\mu\text{M}$ ) in  $\text{CH}_3\text{CN}/\text{H}_2\text{O}$  (9:1, v/v) solution upon addition of increasing concentrations of  $\text{Hg}(\text{ClO}_4)_2$  with an excitation wavelength at 550 nm.



emission could be ascribed to the delocalized xanthene moiety of the rhodamine group.

No significant spectral change of **CRB** occurred in the presence of alkali and alkaline-earth metals, such as  $\text{Na}^+$ ,  $\text{K}^+$ ,  $\text{Mg}^{2+}$ , and  $\text{Ca}^{2+}$ , and the first-row transition metals  $\text{Mn}^{2+}$ ,  $\text{Fe}^{2+}$ ,  $\text{Co}^{2+}$ ,  $\text{Ni}^{2+}$ , and  $\text{Cu}^{2+}$ , and even group 12 metals  $\text{Zn}^{2+}$  and  $\text{Cd}^{2+}$  as well as  $\text{Pb}^{2+}$  and  $\text{Ag}^+$  (Fig. S6, green bars). It is likely that there are a number of combined influences achieving the unique selectivity for the  $\text{Hg}^{2+}$  ion, including the suitable coordination conformation of the bis-chelating Schiff-based receptor, the larger radius of the  $\text{Hg}^{2+}$  ion, the nitrogen-affinity character of the  $\text{Hg}^{2+}$  ion, and the amide deprotonation ability of the  $\text{Hg}^{2+}$  ion.<sup>21</sup> The competitive fluorescent experiment (585 nm) of **CRB** (20  $\mu\text{M}$ ) in  $\text{CH}_3\text{CN}/\text{H}_2\text{O}$  (9:1, v/v) upon addition of different metal cations (0.2 mM as perchlorates) and  $\text{Hg}(\text{ClO}_4)_2$  (0.1 mM) revealed that the Hg-induced luminescence response was exclusive for  $\text{Hg}^{2+}$  and unaffected in the background of environmentally relevant alkali or alkaline-earth metals, including  $\text{Na}^+$ ,  $\text{K}^+$ ,  $\text{Mg}^{2+}$ , and  $\text{Ca}^{2+}$ , the first-row transition-metal ions  $\text{Mn}^{2+}$ ,  $\text{Fe}^{2+}$ ,  $\text{Co}^{2+}$ , and  $\text{Ni}^{2+}$ , and even group 12 metal  $\text{Zn}^{2+}$  and  $\text{Cd}^{2+}$ , as well as  $\text{Pb}^{2+}$  and  $\text{Ag}^+$ , except  $\text{Cu}^{2+}$  ion, which partly quenched the  $\text{Hg}^{2+}$ -induced luminescence of **CRB** (Fig. S6, red bars), through a d–d electron paramagnetic quenching or/and an energy transfer mechanism.<sup>18</sup>

Fluorescent probes for detecting heavy metal, particularly those that have practical application in living cells, has attracted much attention.<sup>22</sup> In view of its good water-solubility, favorable spectroscopic properties, and the instantaneous interaction with mercury ions, **CRB** should be well-suited for fluorescence imaging in living cells. The fluorescence imaging of intracellular  $\text{Hg}^{2+}$  was observed under Nikon eclipse TE2000-5 inverted fluorescence microscopy with a 20 $\times$  objective lens (excited with blue and green light, respectively). As determined by fluorescence imaging experiment (Fig. 5), staining MCF-7 with a 10  $\mu\text{M}$  solution of **CRB** for 15 min at 37  $^\circ\text{C}$  under 5%  $\text{CO}_2$  led to very faint intracellular red fluorescence (excited with 510–570 nm light) and obvious green fluorescence (excited with 460–510 nm light). After rinsed with PBS three times, the cells were supplemented with 20  $\mu\text{M}$   $\text{Hg}^{2+}$  for another 15 min. The obvious bright red fluorescence can be

observed (excited with green light). Before and after addition of mercury ions, the green fluorescence did not change obviously (excited with blue light). It indicates that the green fluorescence of coumarin as donor did not quench after addition of mercury ions, which is coincident with the emission spectrum of **CRB**. The preliminary results indicate that **CRB** is cell-permeable and can realize ratiometric detection of mercury ions in living cells. The further experiments in living cells are still under way.

The response of **CR6G** to  $\text{Hg}^{2+}$  in UV–vis spectra in  $\text{CH}_3\text{CN}/\text{H}_2\text{O}$  (9:1, v/v) was also investigated (Fig. 6a). The new absorption peak at 530 nm ( $\log \epsilon=4.76$ ) appeared and the intensity increased dramatically with each addition of  $\text{Hg}^{2+}$ . The intensity finally remained constant after approximately 5 equiv of  $\text{Hg}^{2+}$  were added. At the same time, the color of solution changed to orange, which can be attributed to the delocalized xanthene moiety of the ring-open amide form of CR6G. The fluorescence enhancement effects of various amounts of  $\text{Hg}^{2+}$  on **CR6G** were investigated under excitation at 500 nm (Fig. 6b). When  $\text{Hg}^{2+}$  was introduced into 20  $\mu\text{M}$  **CR6G** solution, an obvious fluorescence peak was observed and also enhanced upon further addition of  $\text{Hg}^{2+}$ , whereas other metal ions displayed much weaker response. The fluorescence intensity attained constant after the addition of 3.5 equiv  $\text{Hg}^{2+}$ .

In conclusion, a universal system based on FRET mechanism, comprising a coumarin donor and a rhodamine acceptor, was developed for the selective and quantitative sensing of metal ions by regulating FRET from 'off' to 'on'. Through changing the mode of connection and the binding site in this FRET system, the ratiometric detection with high selectivity and sensitivity were realized for different metal ions  $\text{Cu}^{2+}$  and  $\text{Hg}^{2+}$ . **RCs** exhibit significant fluorescence enhancement and excellent selectivity toward  $\text{Cu}^{2+}$  over other competitive ions. Due to the larger spectra overlap between the acceptor and donor of **RC1** than that of **RC2**, the FRET efficiency of **RC1** (90%) is higher than that of **RC2** (33%). Such result would be helpful to design more effective FRET chemosensors. **CRB** and **CR6G** can serve as chemosensors for selective and quantitative detection of  $\text{Cu}^{2+}$  in aqueous media. We anticipate that the construction of this universal FRET system based on coumarin and rhodamine would open a broader prospect of ratiometric fluorescent probes

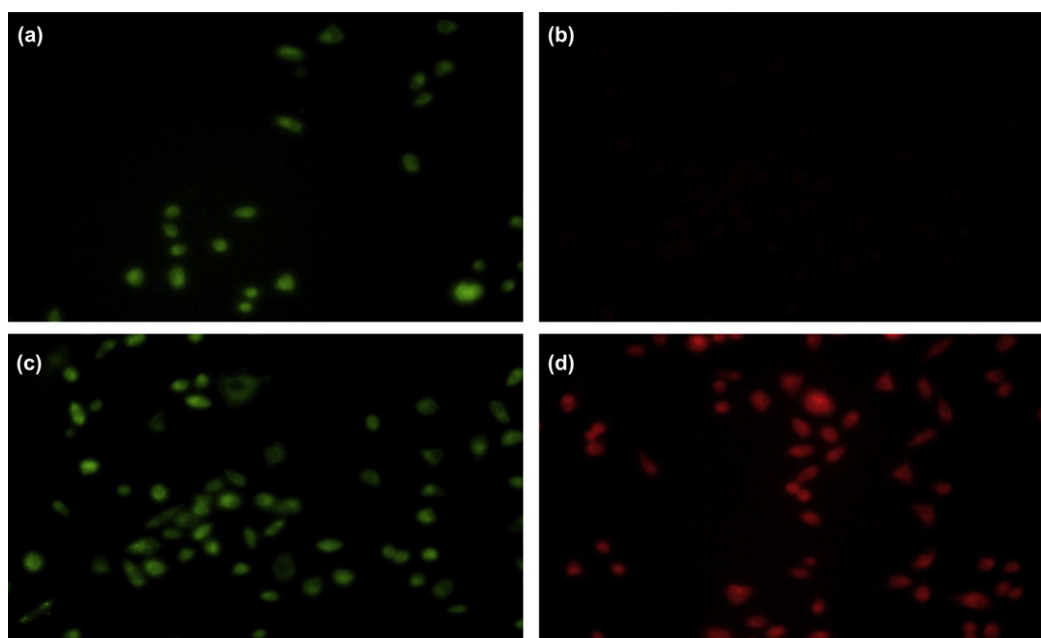


**Fig. 5.** Fluorescence images of MCF-7 (breast cancer) cells. (a) and (c): Fluorescence image of MCF-7 cells incubated with **CRB** excited with blue and green light, respectively. (b) and (d): Fluorescence image of MCF-7 cells incubated with **CRB** for 15 min, washed three times, then incubated with 10  $\mu\text{M}$   $\text{Hg}^{2+}$  for 15 min, excited with blue and green light, respectively.

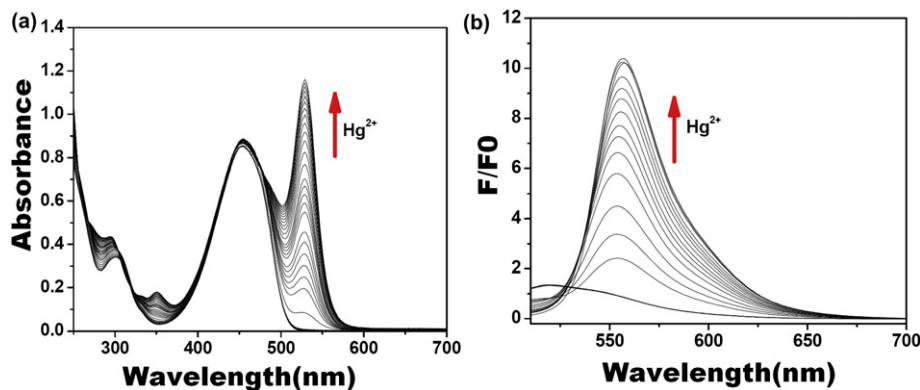


**Fig. 6.** (a) UV–vis spectra of **CR6G** (20  $\mu\text{M}$ ) in  $\text{CH}_3\text{CN}/\text{H}_2\text{O}$  (9:1, v/v) solution upon addition of increasing concentrations of  $\text{Hg}(\text{ClO}_4)_2$ . (b) Fluorescence spectra of **CR6G** (20  $\mu\text{M}$ ) in  $\text{CH}_3\text{CN}/\text{H}_2\text{O}$  (9:1, v/v) solution upon addition of increasing concentrations of  $\text{Hg}(\text{ClO}_4)_2$  with an excitation at 500 nm.

for detecting various other environmentally and biologically important species. At present, further researches are still under way in our laboratory.

## 2. Experimental

### 2.1. Instruments and reagents

The elemental analyses of C, H, and N were performed on a Vario EL III elemental analyzer.  $^1\text{H}$  NMR and  $^{13}\text{C}$  NMR spectra were measured on a Varian INOVA 400 M spectrometer. API mass spectra were recorded on a HP1100LC/MSD spectrometer. ESI mass spectra were carried out on an HPLC–Q-ToF MS spectrometer by using methanol as mobile phase. UV–vis spectra were measured on an HP 8453 spectrometer. The solution fluorescent spectra were measured on Edinburgh F920. For all fluorescent measurements, both excitation and emission slit widths were set as 1 nm. IR spectra were recorded using KBr pellets on a Vector 22 Bruker spectrophotometer in the  $4000\text{--}400\text{ cm}^{-1}$  regions. All cationic compounds such as perchlorate of  $\text{Na}^+$ ,  $\text{K}^+$ ,  $\text{Mg}^{2+}$ ,  $\text{Ca}^{2+}$ ,  $\text{Mn}^{2+}$ ,  $\text{Fe}^{2+}$ ,  $\text{Co}^{2+}$ ,  $\text{Ni}^{2+}$ ,  $\text{Cu}^{2+}$ ,  $\text{Zn}^{2+}$ ,  $\text{Pb}^{2+}$ ,  $\text{Cd}^{2+}$ ,  $\text{Hg}^{2+}$ , and  $\text{Ag}^+$  were obtained from commercial sources and used as received. Acetonitrile for spectrometric detection was HPLC reagent without fluorescent impurity and deionized water was used in the experiment. All the other solvents and reagents were of analytical grade.

### 2.2. General procedures of spectra detection

Stock solutions of **RC1** and **RC2** were prepared in acetonitrile of HPLC grade. Stock solutions of **CRB** and **CR6G** were prepared in  $\text{CH}_3\text{CN}/\text{H}_2\text{O}$  (9:1, v/v). The cationic solutions were all in  $\text{CH}_3\text{CN}$  with a concentration of  $2.0 \times 10^{-2}\text{ M}$  for spectrometric analysis. Excitation wavelength for **RC1** and **RC2** was 415 nm.

Excitation wavelengths for **CRB** and **CR6G** were 420 nm for the fluorescence titration of  $\text{Cu}^{2+}$ . Before spectroscopic measurements, the solution was freshly prepared by diluting the high concentration stock solution to corresponding solution. Each time a 2 mL solution of probe was filled in a quartz cell of 1 cm optical path length, and different stock solutions of cations were added into the quartz cell gradually by using a micro-syringe. The volume of cationic stock solution added was less than 100  $\mu\text{L}$  with the purpose of keeping the total volume of testing solution without obvious change.

### 2.3. Quantum yield measurement

Fluorescence quantum yield was determined using optically matching solutions of rhodamine B ( $\Phi_f=0.69$  in ethanol) as standard at an excitation wavelength of 550 nm.

$$\Phi_{\text{unk}} = \Phi_{\text{std}} \left( \frac{I_{\text{unk}}/A_{\text{unk}}}{I_{\text{std}}/A_{\text{std}}} \right) \left( \frac{\eta_{\text{unk}}}{\eta_{\text{std}}} \right)^2$$

Excitation and emission slit widths were modified to adjust the luminescent intensity in a suitable range. All the spectroscopic measurements were performed at least in triplicate and averaged.

**2.3.1. Compound RC1.** *N*-(Rhodamine-6G)lactam-ethylenediamine<sup>23</sup> (1.14 g, 2.5 mmol) and  $\text{Et}_3\text{N}$  (0.42 mL, 3 mmol) were mixed in  $\text{CH}_2\text{Cl}_2$  (20 mL) under nitrogen. A solution of 7-diethylamino-2-oxo-2H-chromen-3-carboxylic chloride<sup>24</sup> (0.70 g, 2.5 mmol) in  $\text{CH}_2\text{Cl}_2$  (60 mL) was added dropwise to the mixture with stirring for 24 h. Then the organic layer was washed with water (200 mL) and dried over anhydrous  $\text{Na}_2\text{SO}_4$ . The solvent was removed under reduced pressure. And the crude product was purified by column chromatography on alumina (ethyl acetate) to afford 1.44 g of yellow solid **RC1** in 82% yield. Mp 253–255  $^\circ\text{C}$ .  $^1\text{H}$  NMR (400 MHz,  $\text{DMSO}-d_6$ ):  $\delta$  (ppm) 8.56–8.58 (m, 2H, 1H for  $-\text{NH}-$  and 1H for  $\text{ArH}$ ), 7.93 (d, 1H,  $J=7.6\text{ Hz}$ ,  $\text{ArH}$ ), 7.37–7.44 (m, 3H,  $\text{ArH}$ ), 7.02 (d, 1H,  $J=8.0\text{ Hz}$ ,  $\text{ArH}$ ), 6.62 (d, 1H,  $J=8.8\text{ Hz}$ ,  $\text{ArH}$ ), 6.47 (s, 1H,  $\text{ArH}$ ), 6.33 (s, 2H, Xanthene-H), 6.29 (s, 2H, Xanthene-H), 3.38–3.47 (m, 6H, 2H for  $-\text{CH}_2\text{CH}_2-$  and 4H for  $-\text{CH}_2\text{CH}_3$ ), 3.12–3.20 (m, 6H, 2H for  $-\text{CH}_2\text{CH}_2-$  and 4H for  $-\text{CH}_2\text{CH}_3$ ), 1.80 (s, 6H,  $-\text{CH}_3$ ), 1.21–1.28 (m, 12H,  $-\text{CH}_2\text{CH}_3$ ).  $^{13}\text{C}$  NMR (100 MHz,  $\text{DMSO}-d_6$ ):  $\delta$  (ppm) 167.3, 161.9, 161.3, 157.1, 153.6, 152.2, 150.8, 147.5, 147.3, 132.6, 131.4, 130.2, 128.1, 127.3, 123.5, 122.2, 118.2, 109.9, 109.2, 107.5, 104.5, 95.7, 95.5, 64.1, 59.5, 54.5, 44.2, 37.3, 16.9, 14.0, 12.2. API-MS  $m/z$ : 700.3 ( $[\text{M}-\text{H}]^+$ ). Anal. Calcd for **RC1**  $\text{C}_{42}\text{H}_{45}\text{N}_5\text{O}_5$ : C 72.08, H 6.48, N 10.01%. Found: C 71.92, H 6.51, N 9.92%.

**2.3.2. Compound RC2.** Under nitrogen,  $\text{Et}_3\text{N}$  (0.42 mL, 3 mmol) was added into a  $\text{CH}_2\text{Cl}_2$  (20 mL) solution of *N*-(rhodamine B) lactamethylenediamine<sup>23</sup> (1.21 g, 2.5 mmol) and then a solution of 7-diethylamino-2-oxo-2H-chromen-3-carboxylic chloride (0.70 g, 2.5 mmol) in  $\text{CH}_2\text{Cl}_2$  (60 mL) was added dropwise to the solution with stirring for 24 h. Then the organic layer was washed with water (200 mL) and dried over anhydrous  $\text{Na}_2\text{SO}_4$ . The solvent was removed under reduced pressure. The crude product was purified by column chromatography on alumina (ethyl acetate) to afford 1.42 g of yellow solid **RC2** in 78% yield. Mp 305–307  $^\circ\text{C}$ .  $^1\text{H}$  NMR (400 MHz,  $\text{CDCl}_3$ ):  $\delta$  (ppm) 8.59–8.65 (m, 2H, 1H for  $\text{ArH}$  and 1H for  $-\text{NH}-$ ), 7.91 (d, 1H,  $J=8.4\text{ Hz}$ ,  $\text{ArH}$ ), 7.36–7.43 (m, 3H,  $\text{ArH}$ ), 7.06 (d, 1H,  $J=8.4\text{ Hz}$ ,  $\text{ArH}$ ), 6.61 (d, 1H,  $J=7.6\text{ Hz}$ ,  $\text{ArH}$ ), 6.50 (d, 2H,  $J=8.8\text{ Hz}$ , Xanthene-H), 6.45 (s, 1H,  $\text{ArH}$ ), 6.36 (s, 2H, Xanthene-H), 6.27 (d, 2H,  $J=8.8\text{ Hz}$ , Xanthene-H), 3.40–3.46 (m, 6H, 2H for  $-\text{CH}_2\text{CH}_2-$  and 4H for  $-\text{CH}_2\text{CH}_3$ ), 3.25–3.31 (m, 10H, 2H for  $-\text{CH}_2\text{CH}_2-$  and 8H for  $-\text{CH}_2\text{CH}_3$ ), 1.22 (t, 6H,  $J=7.0\text{ Hz}$ ,  $-\text{CH}_2\text{CH}_3$ ), 1.13 (t, 12H,  $J=7.0\text{ Hz}$ ,  $-\text{CH}_2\text{CH}_3$ ).  $^{13}\text{C}$  NMR (100 MHz,  $\text{CDCl}_3$ ):  $\delta$  (ppm) 168.5, 162.8, 162.2, 157.4, 153.7, 153.1, 152.1, 148.6, 147.5,

132.2, 130.9, 130.8, 128.7, 127.8, 123.6, 122.7, 110.6, 109.6, 108.3, 108.1, 105.5, 97.7, 96.4, 64.8, 44.9, 44.1, 39.6, 37.9, 12.5, 12.3. API-MS  $m/z$ : 728.3 ( $[M-H]^+$ ), 750.3 ( $[M-Na]^+$ ). Anal. Calcd for **RC2**  $C_{44}H_{49}N_5O_5$ : C 72.60, H 6.79, N 9.62%. Found: C 72.46, H 6.87, N 9.47%.

**2.3.3. Compound CRB.** Rhodamine B hydrazide<sup>11,25</sup> (1.0 mmol, 0.457 g) and 7-diethylaminocoumarin-3-aldehyde<sup>26</sup> (1.0 mmol, 0.245 g) were mixed in 30 mL methanol with three drops of acetic acid. After the solution was refluxed for 3 h with stirring, yellow precipitates obtained were filtered, washed with methanol (3×5 mL) and dried under vacuum. Yield: 0.52 g (76%). Mp 189–191 °C.  $^1H$  NMR (400 MHz,  $CDCl_3$ ):  $\delta$  (ppm) 8.38 (s, 1H,  $-N=CH_2-$ ), 8.19 (s, 1H, ArH), 8.01 (d, 1H,  $J=6.4$  Hz, ArH), 7.45 (m, 2H, ArH), 7.27 (d, 1H, ArH), 7.08 (d, 1H,  $J=6.4$  Hz), 6.48–6.53 (m, 5H, 4H for Xanthene-H and 1H for ArH), 6.38 (s, 1H, ArH), 6.24 (d, 2H,  $J=8.0$  Hz, Xanthene-H), 3.39–3.39 (m, 12H,  $-CH_2CH_3$ ), 1.30–1.02 (m, 18H,  $-CH_2CH_3$ ).  $^{13}C$  NMR (100 MHz,  $CDCl_3$ ):  $\delta$  (ppm) 165.1, 161.3, 156.8, 153.0, 152.6, 151.0, 149.0, 141.2, 138.3, 133.4, 130.2, 128.4, 128.1, 127.8, 123.7, 123.4, 114.9, 109.1, 108.8, 108.0, 105.5, 98.2, 97.1, 65.8, 44.9, 44.3, 12.6, 12.5. API-MS  $m/z$ : 684.3 ( $[M-H]^+$ ), 706.3 ( $[M-Na]^+$ ). Anal. Calcd for  $C_{42}H_{45}N_5O_4$ : H 6.63, C 73.77, N 10.24%. Found: H 6.62, C 73.66, N 10.20%.

**2.3.4. Compound CR6G.** Rhodamine 6G hydrazide (1.0 mmol, 0.457 g) and 7-diethylaminocoumarin-3-aldehyde (1.0 mmol, 0.245 g) were mixed in 30 mL methanol with three drops of acetic acid. After the solution was refluxed for 3 h with stirring, yellow precipitates obtained were filtered, washed with methanol (3×5 mL), and dried under vacuum. Yield: 0.53 g (81%). Mp 307–308 °C.  $^1H$  NMR (400 MHz,  $CDCl_3$ ):  $\delta$  (ppm) 8.26 (s, 1H,  $-N=CH-$ ), 8.21 (s, 1H, ArH), 8.00 (d, 1H,  $J=7.0$  Hz, ArH), 7.40 (m, 2H, ArH), 7.26 (d, 1H,  $J=8.8$  Hz, ArH), 7.00 (d, 1H,  $J=7.0$  Hz, ArH), 6.51 (d, 1H,  $J=6.8$  Hz, ArH), 6.45 (s, 2H, Xanthene-H), 6.37 (s, 1H, ArH), 6.33 (s, 2H, Xanthene-H), 3.61–3.30 (m, 6H, 2H for  $-NH-$ , 2H for  $-CH_2CH_3$ ), 3.20 (q, 4H,  $J=7.1$  Hz,  $-CH_2CH_3$ ), 1.87 (s, 6H,  $-CH_3$ ), 1.30 (t, 6H,  $J=7.1$  Hz,  $-CH_2CH_3$ ), 1.18 (t, 6H,  $J=7.1$  Hz,  $-CH_2CH_3$ ).  $^{13}C$  NMR (100 MHz,  $CDCl_3$ ):  $\delta$  (ppm) 165.3, 161.3, 156.8, 152.9, 151.2, 151.0, 147.5, 140.6, 138.2, 133.5, 130.2, 128.1, 128.0, 127.4, 123.6, 123.4, 118.0, 114.7, 109.1, 108.8, 106.1, 97.1, 97.0, 65.7, 44.9, 38.4, 16.7, 14.7, 12.5. API-MS  $m/z$ : 656.3 ( $[M-H]^+$ ), 678.3 ( $[M-Na]^+$ ). Anal. Calcd for  $C_{40}H_{41}N_5O_4$ : H 6.30, C 73.26, N 10.68%. Found: H 6.35, C 73.18, N 10.61%.

## Acknowledgements

We gratefully acknowledge financial support from the National Natural Science foundation of China.

## Supplementary data

Supplementary data associated with this article can be found in online version at doi:10.1016/j.tet.2010.09.043.

## References and notes

- (a) Basabe-Desmonts, L.; Reinhoudt, D. N.; Crego-Calama, M. *Chem. Soc. Rev.* **2007**, 36, 993–1017; (b) Gunnlaugsson, T.; Glynn, M.; Tocci, G. M.; Kruger, P. E.; Pfeffer, F. M. *Coord. Chem. Rev.* **2006**, 250, 3094–3117; (c) Nolan, E. M.; Lippard, S. J. *Chem. Rev.* **2008**, 108, 3443–3480; (d) Kim, H. N.; Lee, M. H.; Kim, H. J.; Kim, J. S.; Yoon, J. *Chem. Soc. Rev.* **2008**, 37, 1465–1472.
- (a) Waggoner, D. J.; Bartnikas, T. B.; Gitlin, J. D. *Neurobiol. Dis.* **1999**, 6, 221–230; (b) Valentine, J. S.; Hart, P. J. *Proc. Natl. Acad. Sci. U.S.A.* **2003**, 100, 3617–3622; (c) Mercer, J. F. B. *Trends Mol. Med.* **2001**, 7, 64–69; (d) Strausak, D.; Mercer, J. F. B.; Dieter, H. H.; Stremmel, W.; Multhaup, G. *Brain Res. Bull.* **2001**, 55, 175–185.
- (a) Rae, T. D.; Schmidt, P. J.; Pufahl, R. A.; Culotta, V. C.; O'Halloran, T. V. *Science* **1999**, 284, 805–808; (b) Puig, S.; Thiele, D. J. *Curr. Opin. Chem. Biol.* **2002**, 6, 171–180.
- (a) Yu, M.; Shi, M.; Chen, Z.; Li, F.; Li, X.; Gao, Y.; Xu, J.; Yang, H.; Zhou, Z.; Yi, T.; Huang, C. *Chem.—Eur. J.* **2008**, 14, 6892–6900; (b) Swamy, K. M. K.; Ko, S.-K.; Kwon, S. K.; Lee, H. N.; Mao, C.; Kim, J.-M.; Lee, K.-H.; Kim, J.; Shin, I.; Yoon, J. *Chem. Commun.* **2008**, 5915–5917; (c) Jung, H. S.; Kwon, P. S.; Lee, J. W.; Kim, J. I.; Hong, C. S.; Kim, J. W.; Yan, S.; Lee, J. Y.; Lee, J. H.; Joo, T.; Kim, J. S. *J. Am. Chem. Soc.* **2009**, 131, 2008–2012.
- (a) Kim, S. H.; Kim, J. S.; Park, S. M.; Chang, S.-K. *Org. Lett.* **2006**, 8, 371–374; (b) Zeng, Q.; Cai, P.; Li, Z.; Qin, J.; Tang, B. Z. *Chem. Commun.* **2008**, 1094–1096; (c) Haugland, R. P. *Handbook of Fluorescent Probes and Research Products*, 9th ed.; Molecular Probe: Eugene, 2002; (d) Mashraqui, S. H.; Khan, T.; Sundaram, S.; Ghadigaonkar, S. *Tetrahedron Lett.* **2008**, 49, 3739–3743; (e) Liu, J.; Lu, Y. J. *Am. Chem. Soc.* **2007**, 129, 9838–9839; (f) Jung, H. S.; Park, M.; Han, D. Y.; Kim, E.; Lee, C.; Ham, S.; Kim, J. S. *Org. Lett.* **2009**, 11, 3378–3381.
- Tsien, R. Y.; Poenie, M. *Trends Biochem. Sci.* **1986**, 11, 450–455.
- (a) Royzen, M.; Dai, Z.; Canary, J. W. *J. Am. Chem. Soc.* **2005**, 127, 1612–1613; (b) Guliyev, R.; Coskun, A.; Akkaya, E. U. *J. Am. Chem. Soc.* **2009**, 131, 9007–9013; (c) Lee, S. Y.; Kim, H. J.; Wu, J.-S.; No, K.; Kim, J. S. *Tetrahedron Lett.* **2008**, 49, 6141–6144; (d) Xu, Z.; Qian, X.; Cui, J. *Org. Lett.* **2005**, 7, 3029–3032; (e) Guo, Z.; Zhu, W.; Shen, L.; Tian, H. *Angew. Chem., Int. Ed.* **2007**, 46, 5549–5553; (f) Yu, H.; Fu, M.; Xiao, Y. *Phys. Chem. Chem. Phys.* **2010**, 12, 7386–7391.
- (a) van der Meer, B. W.; Coker, G.; Simon, S. Y. *Resonance Energy Transfer, Theory and Data*; VCH: Weinheim, 1994; (b) Adams, S. R.; Harootunian, A. T.; Buechler, Y. J.; Taylor, S. S.; Tsien, R. Y. *Nature* **1991**, 349, 694–697; (c) Sapsford, K. E.; Berti, L.; Medintz, I. L. *Angew. Chem., Int. Ed.* **2006**, 45, 4562–4588; (d) Zhang, X.; Xiao, Y.; Qian, X. *Angew. Chem., Int. Ed.* **2008**, 47, 8025–8029; (e) Lee, M. H.; Mingsha, D. T.; Jung, H. S.; Yoon, J.; Lee, C.-H.; Kim, J. S. *J. Org. Chem.* **2007**, 72, 4242–4245; (f) Zhou, Z.; Yu, M.; Yang, H.; Huang, K.; Li, F.; Yi, T.; Huang, C. *Chem. Commun.* **2008**, 3387–3389; (g) Jung, J. H.; Lee, M. H.; Kim, H. J.; Jung, H. S.; Lee, S. Y.; Shin, N. R.; No, K.; Kim, J. S. *Tetrahedron Lett.* **2009**, 50, 2013–2016.
- (a) Förster, T. *Ann. Phys.* **1948**, 2, 55–75; (b) Berberan-Santos, M. N.; Choppinet, P.; Fedorov, A.; Jullien, L.; Valeur, B. *J. Am. Chem. Soc.* **2000**, 122, 11876–11886; (c) Burghart, A.; Thoresen, L. H.; Chen, J.; Burgess, K.; Bergström, F.; Johansson, L. B.-Å. *Chem. Commun.* **2000**, 2203–2204; (d) Albers, A. E.; Okregal, V. S.; Chang, C. J. *J. Am. Chem. Soc.* **2006**, 128, 9640–9641; (e) Suresh, M.; Mishra, S.; Mishra, S. K.; Suresh, E.; Mandal, A. K.; Shrivastav, A.; Das, A. *Org. Lett.* **2009**, 11, 2740–2743.
- (a) Mizukami, S.; Watanabe, S.; Hori, Y.; Kikuchi, K. *J. Am. Chem. Soc.* **2009**, 131, 5016–5017; (b) Mizukami, S.; Okada, S.; Kimura, S.; Kikuchi, K. *Inorg. Chem.* **2009**, 48, 7630–7638; (c) Zheng, H.; Qian, Z.; Xu, L.; Yuan, F.; Lan, L.; Xu, J. *Org. Lett.* **2006**, 8, 859–861; (d) Wu, J.; Hwang, I.; Kim, K. S.; Kim, J. S. *Org. Lett.* **2007**, 9, 907–910; (e) Shi, W.; Ma, H. *Chem. Commun.* **2008**, 1856–1858; (f) Lee, M. H.; Kim, H. J.; Yoon, S.; Park, N.; Kim, J. S. *Org. Lett.* **2008**, 10, 213–216; (g) Kim, M. H.; Jang, H. H.; Yi, S.; Chang, S.-K.; Han, M. S. *Chem. Commun.* **2009**, 4838–4840.
- (a) Dujols, V.; Ford, F.; Czarnik, A. W. *J. Am. Chem. Soc.* **1997**, 119, 7386–7387; (b) Huang, W.; Song, C.; He, C.; Lv, G.; Hu, X.; Zhu, X.; Duan, C. *Inorg. Chem.* **2009**, 48, 5061–5072.
- (a) Xiang, Y.; Tong, A. *Org. Lett.* **2006**, 8, 1549–1552; (b) Yang, H.; Zhou, Z.; Huang, K.; Yu, M.; Li, F.; Yi, T.; Huang, C. *Org. Lett.* **2007**, 9, 4729–4732; (c) Jana, A.; Kim, J. S.; Jung, H. S.; Bharadwaj, P. K. *Chem. Commun.* **2009**, 4417–4419; (d) Xiang, Y.; Tong, A.; Jin, P.; Ju, Y. *Org. Lett.* **2006**, 8, 2863–2866; (e) Othman, A. B.; Lee, J. W.; Wu, J. S.; Kim, J. S.; Abidi, R.; Thuéry, P.; Strub, J. M.; Dorselaer, A. V.; Vicens, J. *J. Org. Chem.* **2007**, 72, 7634–7640.
- He, G.; Guo, D.; He, C.; Zhang, X.; Zhao, X.; Duan, C. *Angew. Chem., Int. Ed.* **2009**, 48, 6132–6135.
- Rogers, J. E.; Weiss, S. J.; Kelly, L. A. *J. Am. Chem. Soc.* **2000**, 122, 427–436.
- Lakowicz, J. R. *Principles of Fluorescence Spectroscopy*, 2nd ed.; Kluwer Academic/Plenum: New York, NY, 1999, Chapter 13.
- (a) Yang, Y. K.; Yook, K. J.; Tae, J. *J. Am. Chem. Soc.* **2005**, 127, 16760–16761; (b) Ko, S. K.; Yang, Y. K.; Tae, J.; Shin, I. *J. Am. Chem. Soc.* **2006**, 128, 14150–14155.
- Lee, M. H.; Wu, J.-S.; Lee, J. W.; Jung, J. H.; Kim, J. S. *Org. Lett.* **2007**, 9, 2501–2504.
- (a) De Silva, A. P.; Gunaratne, H. Q. N.; Gunnlaugsson, T.; Huxley, A. J. M.; McCoy, C. P.; Rademacher, J. T.; Rice, T. E. *Chem. Rev.* **1997**, 97, 1515–1566; (b) Li, Y.; Yang, C. M. *Chem. Commun.* **2003**, 2884–2885; (c) Fabbri, L.; Licchelli, M.; Pallavicini, P.; Perotti, A.; Taglietti, A.; Sacchi, D. *Chem.—Eur. J.* **1996**, 2, 75–82; (d) Varnes, A. W.; Dodson, R. B.; Wehry, E. L. *J. Am. Chem. Soc.* **1972**, 94, 946–950; (e) Xu, Z.; Kim, S.; Kim, H. N.; Han, S. J.; Lee, C.; Kim, J. S.; Qian, X.; Yoon, J. *Tetrahedron Lett.* **2007**, 48, 9151–9154.
- Anthoni, U.; Christophersen, C.; Nielsen, P. H.; Püschel, A.; Schaumburg, K. *Struct. Chem.* **1995**, 3, 161–165.
- Kwon, J. Y.; Jang, Y. J.; Lee, Y. J.; Kim, K. M.; Seo, M. S.; Nam, W.; Yoon, J. *J. Am. Chem. Soc.* **2005**, 127, 10107–10111.
- He, G.; Zhao, Y.; He, C.; Liu, Y.; Duan, C. *Inorg. Chem.* **2008**, 47, 5169–5176.
- (a) Que, E. L.; Domaille, D. W.; Chang, C. J. *Chem. Rev.* **2008**, 108, 1517–1549; (b) Yoon, S.; Miller, E. W.; He, Q.; Do, P. H.; Chang, C. J. *Angew. Chem., Int. Ed.* **2007**, 46, 6658–6661.
- Zhang, X.; Shiraishi, Y.; Hirai, T. *Org. Lett.* **2007**, 9, 5039–5042.
- Ma, Y.; Luo, W.; Quinn, P. J.; Liu, Z.; Hider, R. C. *J. Med. Chem.* **2004**, 47, 6349–6362.
- Yang, X.-F.; Guo, X.-Q.; Zhao, Y.-B. *Talanta* **2002**, 57, 883–890.
- Wu, J.; Liu, W.; Zhuang, X.; Wang, F.; Wang, P.; Tao, S.; Zhang, X.; Wu, S.; Lee, S. *Org. Lett.* **2007**, 9, 33–36.